Self-Sorted, Random and Block Supramolecular Co-polymers via Sequence Controlled, Multicomponent Self-Assembly

Aritra Sarkar,[§] Ranjan Sasmal,[§] Charly Empereur-mot,[†] Davide Bochicchio,[†] Srinath V. K. Kompella,[∂] Kamna Sharma,[§] Shikha Dhiman,[§] Balasubramanian Sundaram,*[,∂] Sarit S. Agasti, *[,§,∂] Giovanni M. Pavan*[,†,‡] and Subi J. George*[,§]

[§] New Chemistry Unit and School of Advanced Materials (SAMAt), Jawaharlal Nehru Centre for Advanced Scientific Research (JNCASR), Jakkur, Bangalore, India-560064.

[†] Department of Innovative Technologies, University of Applied Sciences and Arts of Southern Switzerland, Galleria 2, Via Cantonale 2c, CH-6928 Manno, Switzerland.

[‡] Department of Applied Science and Technology, Politecnico di Torino, Corso Duca degli Abruzzi24, 10129 Torino, Italy.

[∂] Chemistry and Physics of Materials Unit, Jawaharlal Nehru Centre for Advanced Scientific Research (JNCASR), Jakkur, Bangalore 560064, India.

ABSTRACT: Multicomponent supramolecular co-polymerization promises to construct complex nanostructures with emergent properties. However even with two monomeric components, various possible outcomes such as self-sorted supramolecular homopolymers, a random (statistical) supramolecular co-polymer, an alternate supramolecular co-polymer or a complex supramolecular block co-polymer can occur, determined by their intermolecular interactions and monomer exchange dynamics and hence structural prediction is extremely challenging. Herein, we target this challenge and demonstrate unprecedented two-component sequence controlled supramolecular co-polymerization by manipulating thermodynamic and kinetic routes in the pathway complexity of self-assembly of the constitutive monomers. Extensive molecular dynamics simulations provided useful mechanistic insights into the monomer exchange rates and free energy of interactions between the monomers that dictate the self-assembly pathway and sequence. Fluorescent nature of core-substituted naphthalene diimide monomers has been further utilized to characterize the three sequences via Structured Illumination Microscopy (SIM).

Introduction

Sequence controlled polymerization is a vital phenomenon observed in natural systems. The genetic information is encoded by nucleobase sequences in DNA and protein's structure and function is determined by its amino acid sequence.[1] This sequence-control has been implemented in covalent polymers via elegant synthetic strategies resulting in emergent structural properties and multitude of applications.[2] On the other hand, supramolecular polymers, composed of dynamic non-covalent interactions between monomers, with predictive sequence would provide an opportunity to dynamically rearrange/reconfigure the composition similar to natural systems.[3] However, supramolecular polymerization with even two components is challenging and the sequence outcome could be either narcissistically self-sorted supramolecular homopolymers (AAA and BBB), random (statistical) supramolecular co-polymer (AABABB), alternate supramolecular co-polymer (ABABAB) or complex supramolecular block co-polymer (AABBAA) whose sequence is determined by the free energy of intermolecular (homo AA, BB vs. hetero AB) interactions, monomer structure and monomer exchange dynamics. In this study, we have demonstrated an unprecedented two-component sequence controlled supramolecular co-polymerization into the three unique sequences by exploiting the delicate balance between the kinetic and thermodynamic parameters of self- assembly. We further manipulate these parameters

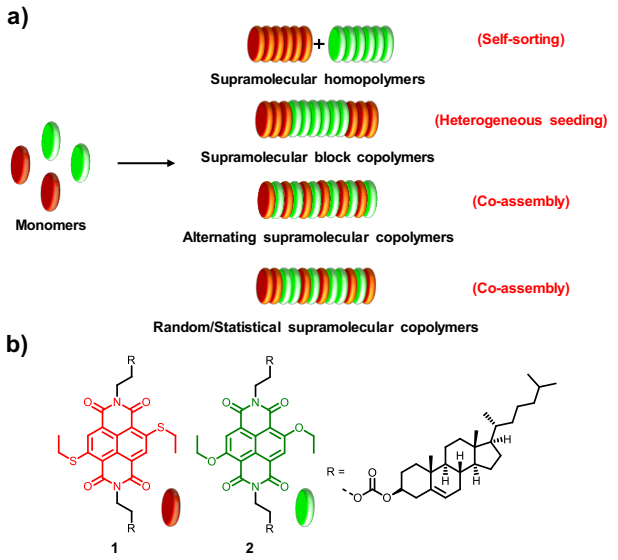

Scheme 1. Two-component supramolecular polymerization. (a) Schematic representation of two-component supramolecular polymerization into narcissistically self-sorted supramolecular homo polymers, heterogeneously seeded supramolecular block co-polymers and co-assembled supramolecular random or alternate co-polymers. (b) Molecular structures of **1** and **2** used for the two-component supramolecular polymerization.

to illustrate dynamic reconfiguration of these sequences into one another.

Narcissistically self-sorted supramolecular polymers have been achieved by high homorecognition (AA, BB > AB) between monomers, designed with structural mismatch or low monomer exchange dynamics.[4-7] Adams and coworkers reported pH-programmed self-sorting of gelator monomers with different pK_a.[5] On the other hand structural mismatch between donor and acceptor chromophores leading to orthogonal supramolecular homopolymers have been reported.[6] We have reported that chirality driven mismatch can also be used to construct self-sorted systems even with structurally similar monomers.[7] In contrast, alternating supramolecular co-polymers require stronger heterorecognition between monomers (AA, BB < AB) and has been preferentially attained by strong heterocomplementary interactions such as electrostatic and donor-acceptor charge-transfer interactions. Charge-transfer supramolecular polymers reported by our group, Zhang and others are excellent examples of alternating supramolecular polymers with electronically complementary donor and acceptor monomers.[8] Besenius and coworkers employed complementary electrostatic interactions from lysine and glutamic acid residues to obtain alternating arrangement at neutral pH.[9] Scherman and coworkers has utilized strong charge-transfer ternary complexes with cucurbit[8]uril to manifest alternate host-guest supramolecular polymer.[10] These self-sorted or alternating supramolecular co-polymers have been achieved mostly under thermodynamic conditions, where the interaction energies between the monomers determines the sequence.

However supramolecular block co-polymer arrangement has been a grand challenge in the field.[11] This is due to specific requirements such as structural similarity between monomers, low exchange dynamics and delicate balance between homo- and hetero-recognition between monomers. However, mechanistic understanding[12] and development of living supramolecular polymerization has aided in addressing this challenge.[11b,13,14] Meijer and coworkers have constructed supramolecular block co-polymers under thermodynamic control with monomers exhibiting reactivity ratio difference analogous to the synthesis of block co-polymers via chain-growth polymerization in covalent polymers.[15] In another approach Yagai and coworkers have demonstrated co-assembly between two monomers under thermodynamic control to result in a supramolecular copolymer, where the monomer composition varies gradually during the polymerization and along the polymer chain.[16] Supramolecular block co-polymerization under kinetic control requires sequential addition of dormant monomers undergoing nucleation-elongation growth. However, this is challenging, as minor difference in structure alters the energy landscape significantly. Hence, Sugiyasu and Takeuchi's group[17] achieved block sequence by crystallization-driven self-assembly approach similar to Manners and coworkers elegantly established in block copolymer assemblies.[18] Aida and coworkers synthesized p-n junction via seeded assembly between electronically different chromophores.[19] Recently, Würthner and coworkers presented the synthesis of supramolecular co-polymers of core-substituted perylene bisimide using kinetically controlled seeded supramolecular polymerization which is more closer to the conventional multicomponent living polymerization leading to block co-polymers.[20]

So far, the narcissistically self-sorted homopolymers, random and block co-polymer sequences have been synthesized separately owing to their orthogonal and unique requisites. Thus, achieving the three sequences from the same monomer pair and their dynamic reconfiguration is still elusive. In order to achieve precise sequence control, it is necessary to move through the complete energy landscape of self-assembly via thermodynamic and kinetic routes. To realize this, herein we introduce an unprecedented two-component supramolecular polymerization with sequence control to access narcissistically self-sorted, random and block co-polymer arrangement via pathway complexity (Scheme 1a, Figure 3d).[21]

To attempt this, we chose our previously studied molecular design based on carbonate cholesterol appended naphthalene diimide (NDI)[22] which due to long-range dipole-dipole interactions followed a cooperative mechanism, necessary for seeded supramolecular polymerization. Secondly, to have minimum structural perturbation and to probe the polymerization process, we symmetrically disubstituted the naphthalene diimide core with ethane thiol (**1**) and ethoxy (**2**) groups to give red and green emissive dyes respectively (Scheme 1b). These molecules have unique optoelectronic properties as well as different absorption and emission profiles aiding to the orthogonal

probing of their self-assembly via spectroscopic and super-resolved florescence microscopy characterization (SIM).[24]

Supramolecular Polymerization of 1 and 2

Core-substituted NDI (cNDI) monomers **1** and **2** have distinct absorption (450-600 nm and 400-500 nm, respectively) and emission profiles (570-750 nm and 450-570 nm, respectively), which allowed the orthogonal probing of its self-assembly characteristics (Figure S1-S3). Supramolecular polymerization of these monomers could be induced in the toluene-MCH solvent mixture (1 % toluene/MCH 8 % toluene in MCH for **1** and 5 % toluene in MCH to 40 % toluene in MCH for **2**) and was probed spectroscopically. **1** and **2** formed red (λ_{max} = 625 nm) and green (λ_{max} = 480 nm) emissive, one-dimensional supramolecular polymers respectively as evident from the structured illumination microscopy (SIM) and transmission electron microscopy (TEM) images (5 % toluene in MCH, Figure 1a,b, S3). Detailed absorption, steady-state and time-resolved fluorescence and excitation spectroscopy studies further revealed J-type slipped organization of chromophores in these stacks. The monomer **2**, in addition to its green emission from self-assembled chromophores, also showed a weak, static excimer emission in the red wavelength region with a maximum at 634 nm (Figure S2c,d). Further, both cNDI chromophores are organized in a helical manner, as evident from the exciton coupled circular dichroism spectra (Figure S1c, S2b), biased by the peripheral chiral cholesterol groups.[23] The good spectral overlap between the absorption spectrum of **1** and emission spectrum of **2**, further enables the probing of the co-polymerization process via Förster Resonance Energy Transfer (FRET) (Figure S4).

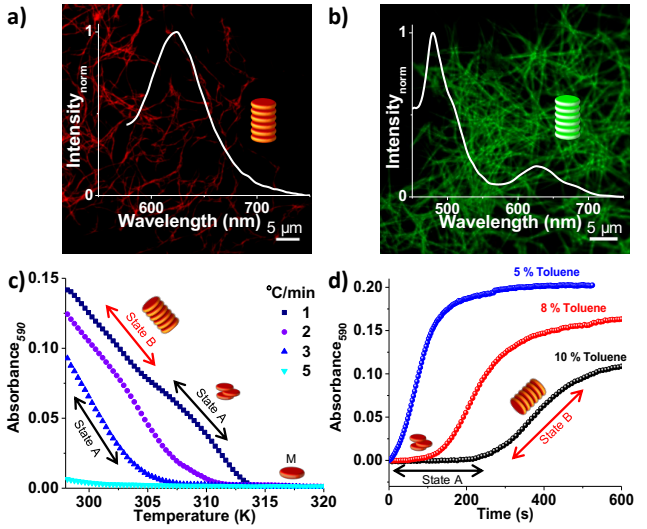

Figure 1. Self-assembly of **1** and **2**. (a) and (b) Emission spectra of **1** (λ_{ex} = 480 nm) and **2** (λ_{ex} = 442 nm) showing fluorescent assembled state with corresponding SIM image showing red (channel I) and green (channel II) fluorescent one-dimensional fibers (5 % toluene/MCH). (c) Temperature dependent absorbance changes at 590 nm with varying cooling rate. An increase in cooling rate leads to the preferential formation of kinetic trapped **State A** over thermodynamically stable **State B** (8 % toluene/MCH). (d) Time-dependent absorption changes at 590 nm of a fast cooled (5 K/min) solution of **1** from 363 K to 298 K depicting self-assembly of **1** into **State B** via sigmoidal nucleation-elongation kinetics. ([**1**] = [**2**] = 5×10^{-5} M, l = 10 mm, black arrow indicates range over **State A** forms and red arrow indicates range which **State B** persists).

Pathway complexity of 1 and 2:

Temperature and time-dependent spectroscopic analyses of **1** and **2** in various toluene/MCH solvent mixtures provided mechanistic insights into the supramolecular polymerization process and the free-energy landscapes. Interestingly, temperature-dependent cooling curves of **1** (363 K to 298 K) recorded at 1 K/min and monitored at 590 nm absorption band (5 % toluene/MCH and 5×10^{-5} M), depicted a two-state transition corresponding to a gradual conversion of monomer to an intermediate self-assembled **State A** finally to the self-assembled **State B**, corresponding to the supramolecular polymeric state (Figure 1c, S5). **State A** was stabilized more in higher toluene percentages (10 and 8 % of toluene) and further, a fast cooling (≥ 5 K/min, ≥ 5 % toluene/MCH) resulted in exclusive formation of **State A** (Figure 1c, S6). Interestingly, self-assembled **State A** transformed to final **State B** with time and time-dependent absorbance changes monitored at 590 nm showed a non-linear, sigmoidal transformation with a lag phase and nucleation-elongation growth mechanism (Figure 1d, S7-S10). An increasing percentage of toluene followed an enhancement in t_{lag} (lag time) and t_{50} (time required for completion of 50 % of the process) due to more stabilization of **State A** at higher percentage of toluene. Also, the presence of hysteresis between the cooling and heating profiles (Figure S6b) indicated **State A** to be a non-equilibrium metastable state *en route* to the thermodynamically stable **State B** of the supramolecular polymer.

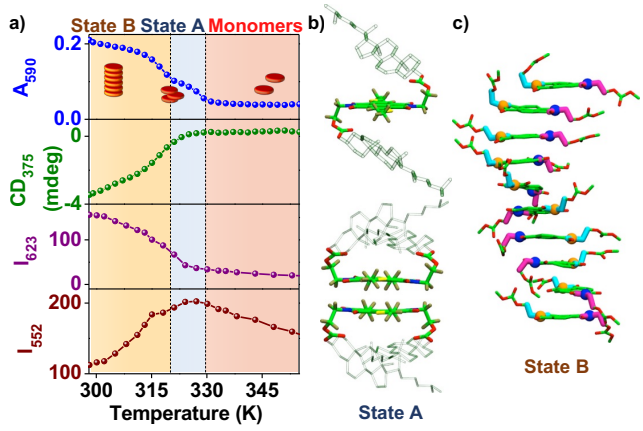

Figure 2. Characterization of metastable **State A** and thermodynamically stable **State B**. (a) Comparison of absorbance at 590 nm, CD at 375 nm and emission changes (λ_{ex} = 480 nm) at 623 nm and 552 nm against temperature. Absorbance and emission at 552 nm show two-step transition. The pink regime indicates molecularly dissolved state, blue region shows the region where **State A** occurs and the orange region shows conversion to final thermodynamically stable **State B**. (b) Side view of the metastable locked chair conformation (top) and side view of the locked dimer conformation (bottom) optimized at the PM6 // BLYP-D3/DZVP level of theory (**State A**)

and (c) snapshot of chair decamer obtained from MD simulations (**State B**). Cholesterol hydrogens are not shown for clarity. ([**1**] = [**2**] = 5×10^{-5} M, 3 % toluene/MCH)

To get further insight into the pathway selectivity in the self-organization of **1** and the metastable **State A**, we further performed concentration and temperature-dependent spectroscopic studies and Molecular Dynamics (MD) simulations. The formation of **State A** resulted in insignificant changes in absorption and emission spectra compared to monomeric state and remains CD inactive, suggesting the formation of less-ordered small aggregates or a conformationally locked, metastable states for the monomers of **1** prior to the nucleation process (Figure 2a, S5). The transition to **State B** was accompanied with a significant broadening of the absorption spectrum and appearance of the new red-shifted aggregate absorption band at 590 nm and the emission band at 625 nm implying the formation of an extended self-assembled structure with exciton-coupled π-stacked chromophores. Gas phase quantum chemical calculations and all-atom molecular dynamic simulations with explicit solvation suggested the formation of locked monomers and dimers as **State A**, which convert to extended supramolecular polymers (**State B**) via conformational changes in the monomer structure (Figure 2b-c). Interestingly, molecule **2** also shows a similar hysteresis and kinetically controlled nucleation-elongation growth at higher solvent percentages of good solvent, toluene (>30 % toluene/MCH) (Figure S12-S14). A decrease in lag time with an increase in the concentration of monomers designates an on-pathway formation of **State A** (Figure S9).

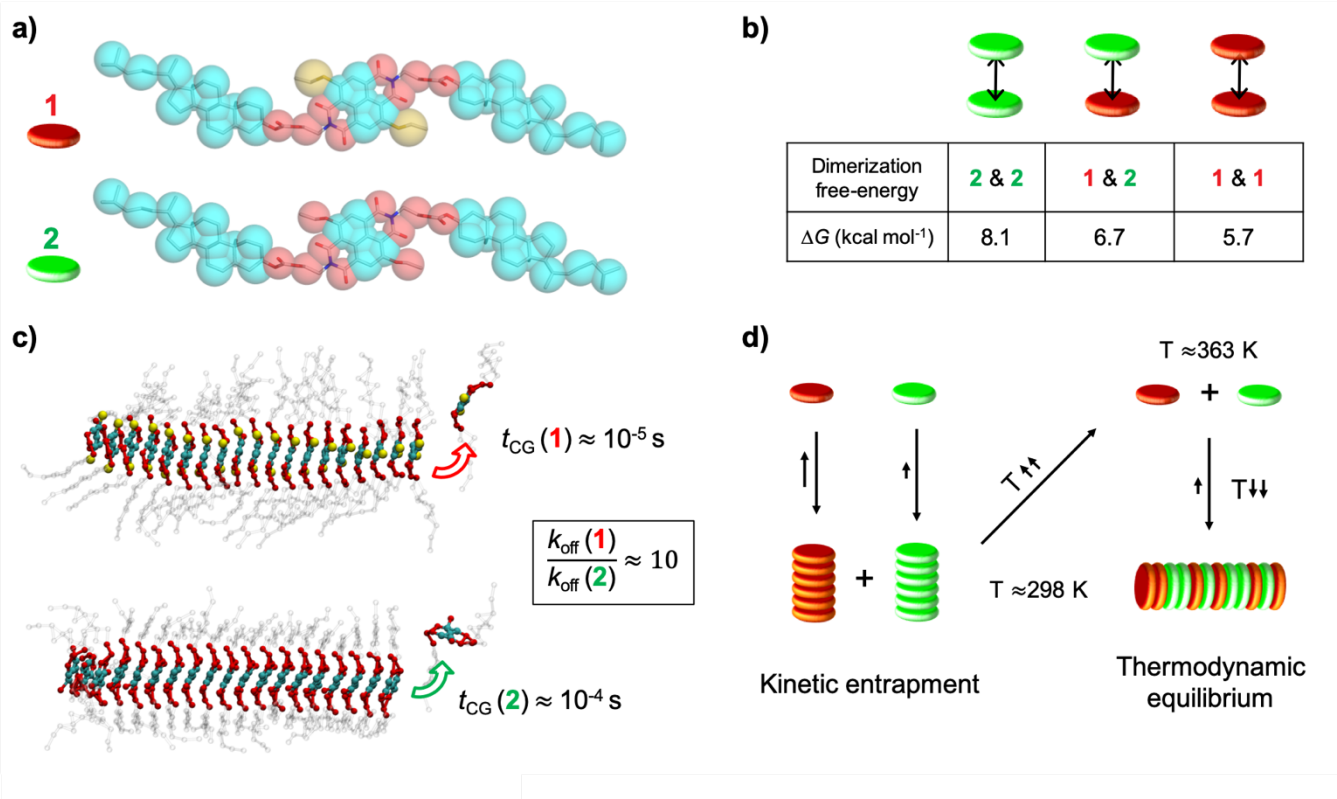

Figure 3. Coarse-grained (CG) molecular simulations of systems **1** and **2**. (a) CG models of monomers **1** and **2** (resolution of the CG models ~5Å). (b) The dimerization free-energies, ΔG, obtained from WT-MetaD simulations allow to compare the strength of monomer-monomer interactions (**1-1** *vs.* **1-2** *vs.* **2-2**). (c) Infrequent WT-MetaD simulations exploring the mechanism and kinetics of monomer exchange form the tips of fibers **1** and **2**. Monomer exchange is found to be ~10 times faster in fiber **1** than in fiber **2**. (d) Model for the formation of blocks of **1** and **2** at room temperature (~298 K: kinetically trapped state), while increasing the temperature to ~90°C (~363 K) moves the equilibrium toward the monomers, which then tend to self-assemble in a random fashion.

Fibers stability and monomer exchange kinetics of 1 vs. 2:

Molecular simulations are extremely useful to obtain a molecular level understanding of dynamic supramolecular polymers.[25,26,27] In particular, by combining fine coarse-grained (CG) models and enhanced sampling approaches it is possible to explore the monomer-monomer interactions, the monomer exchange kinetics and the relative stability of assemblies.[17,28] Hence we have built fine CG models for monomers **1** and **2** (having resolution ~5Å), which are shown in Figure 3a. Using the same approach used recently for modeling similar supramolecular assemblies,[17,25-28] the CG models, which are based on the MARTINI CG force field,[25] have been then refined in order to be consistent with the behavior of the systems seen at the all-atom level

(see Computational Methods in the Supporting Information for details). We used well-tempered metadynamics (WT-MetaD) simulations[30] to explore the stacking/destacking of monomers in explicit cyclohexane solvent molecules (equivalent to MCH at the level of resolution of the CG models used herein).REF This allowed us to compare the free-energy of binding between different monomers, *i.e.* **1-1** *vs.* **1-2** *vs.* **2-2** (see table in Figure 3b). The **2-2** interaction (8.1 kcal mol^{-1}) was found to be stronger than the mixed **1-2** interaction (6.7 kcal mol^{-1}) and of the **1-1** interaction (5.7 kcal mol^{-1}). Accordingly, fiber **1** was found to be more dynamic than fiber **2**. Starting from pre-equilibrated stacks containing 20 monomers of **1** or **2**, we used infrequent WT-MetaD simulations to activate and study the event of monomer exchange from the tips of the two fibers.[17,28] At this scale, the exchange of monomers out from the assemblies is a rare event, the kinetics of which can be reliably reconstructed from multiple biased WT-MetaD exchange runs (see also Methods in the SI).[17,28,31,32] These simulations provided characteristic monomer exchange timescales (t_{CG}) in the order of ~10^{-4} s for fiber **2** *vs.* ~10^{-5} s for fiber **1** (Figure 3c). While these exchange timescales are obtained from approximated CG models, and should be thus considered qualitatively, these still maintain a useful comparative value, indicating that the monomer exchange rate (k_{off}, which can be calculated as $1/t_{CG}$) is ~10 times faster in fiber **1** than in fiber **2**. Altogether, these data allowed us to propose the scheme for the formation of block *vs.* random supramolecular polymers of **1** and **2** as shown in Figure 3d. At room temperature (298 K) monomer exchange in/out these fibers is rare and fibers **1** and fibers **2** tend

Figure 4

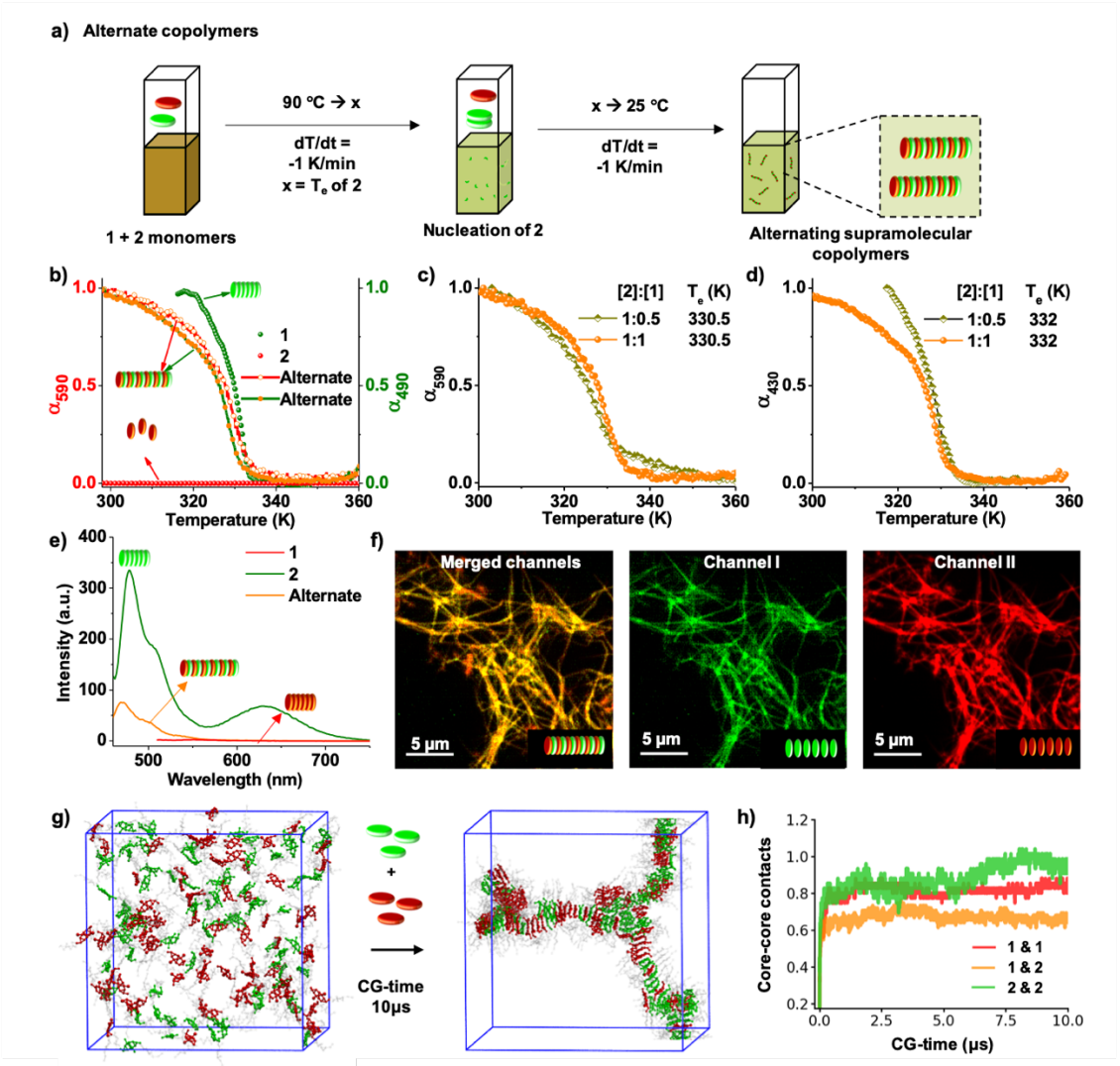

Figure 4. Experimental and simulation studies of supramolecular random co-polymers. (a) Schematic representation showing the preparation of random supramolecular co-polymer under thermodynamic control. (b) Cooling curves of homopolymers of **1** and **2** and the copolymer, showing heterogeneous nucleation under thermodynamic control, with nucleation and growth of **1** on *in situ* formed nuclei of **2**, when monitored at aggregated band of **1**. ([**1**] = [**2**] = 2.5×10^{-5} M). Temperature dependent cooling curves of (c), (d) co-assembled solution of **1** and **2** keeping the concentration of **2** constant and with varying concentrations of **1**, which shows a

constant T_e when monitored (c) at 590 nm (corresponds to aggregate band of **1**) and (d) at 490 nm (corresponds to aggregate band of **2**) showing formation of nuclei of **2**, followed by the growth of both **1** and **2** to form an random co-polymer. ([**2**] = 2.5×10^{-5} M). (e) Quenched donor emission with the absence of excimer band depicting the formation of supramolecular random co-polymers. (λ_{ex} = 442 nm, l = 10 mm) (f) SIM image displaying completely overlapping red and green emission from **1** and **2** respectively confirming the formation of supramolecular random co-polymers. ([**1**] = [**2**] = 2.5×10^{-5} M, 5 % toluene/MCH). (g) Self-assembly of **1** and **2** monomers (75 + 75) during 10 μs of CG-MD. During the run, the **1** and **2** monomers mix randomly together, in the form of short red and green segments and monomers suggesting the formation of random supramolecular copolymers. (h) Number of contacts between the centers of the red-red (red), green-green (green) and green-red (yellow) monomer cores in the system during the CG-MD – similar contacts between the yellow *vs.* red and green lines identify intermixing between the monomers. (Channel I: λ_{ex} = 488 nm, λ_{coll} = 495–575; Channel II: λ_{ex} = 561 nm, λ_{coll} = 570–650).

to bind between them forming non-dynamic and stable blocks (the interaction **1-2** is quite strong). However, when temperature is increased to 363 K, the equilibrium moves toward the monomers and hence fibers **1** and **2** disassemble with time. From such a disassembled state, the mixing of monomers then become quite random, consistent with the rather similar **1-1** *vs.* **1-2** *vs.* **2-2** monomer-monomer interactions (Figure 3b, table). This has been supported by means of experiments and self-assembly simulations (*vide infra*).

Controlled supramolecular polymerization:

As discussed above, during a two-component supramolecular polymerization, there are many possible outcomes: formation of supramolecular homopolymers (narcissistic self-sorting), supramolecular random co-polymer, supramolecular alternate co-polymer, and supramolecular block co-polymer (Scheme 1). Based on the essential requirements as mentioned above, we thought of using molecules **1** and **2** exhibiting kinetically controlled growth and low structural mismatch for a sequence controlled supramolecular polymerization. By exploiting, thermodynamic and kinetic routes of sample preparation and the molecular level insight obtained from MD simulations of monomer exchange dynamics and interaction energies, we envisage to obtain the structurally distinct supramolecular polymers by utilizing the same molecules. We use extensive spectroscopic and microscopic probing and MD simulations to characterize these sequence-controlled supramolecular assemblies.

Random Supramolecular Co-polymers under Thermodynamic Control

First, we investigated the temperature-dependent supramolecular co-polymerization of an equimolar mixture of **1** and **2** monomers, by slowly cooling (1 K/min) from 363 K to 298 K (Figure 4). The growth process of both **1** and **2** can be selectively probed by monitoring their aggregation band at 590 nm and 490 nm, respectively. Supramolecular homopolymerization of individual monomers (2.5×10^{-5} M) in 5 % toluene/MCH solvent mixture, by cooling at a rate of 1 K/min, showed distinct self-assembling behavior. Monomer **1** gets trapped in the metastable **State A**, whereas **2** undergoes a cooperative supramolecular polymerization with an elongation temperature (T_e) of 332±1 K (Figure S15a). Thus, we envisage that, on supramolecular co-polymerization, strong homo-recognition between monomers **1** and **2** would lead to self-sorted supramolecular homopolymers, while strong hetero-recognition between the monomers would be required to construct supramolecular random co-polymers. Temperature-dependent supramolecular co-polymerization of 1:1 mixture of **1** and **2** from 363 K to 298 K at 1 K/min showed cooperative growth of both **1** and **2** (when monitored exclusively at their individual aggregation bands) with identical T_e of 332±1 K. This matches well with the T_e of temperature dependent assembly of pure **2** (Figure 4b) suggesting the co-assembly of monomers. At a constant concentration of **2**, the variation of concentration of **1** did not result in any change in their elongation temperature (Figure 4c,d, S16). Further, the variation of monomer composition (**1**:**2** ratio) while keeping the total concentration at 2.5×10^{-5} M showed a change in T_e proportionally with the concentration of **2** (Figure S17) and matched well with the T_e of pure **2** of similar concentrations. These observations hint towards the heterogeneous nucleation of monomers of **1** triggered by **2**, rather than the cooperative growth of a hetero-dimer, which would have resulted in maximum T_e at 1:1 monomer composition. However, the resultant solution showed a new CD spectrum different from individual components with no bisignation at the absorption maximum of **2**, elucidating a random arrangement of monomers rather than blocky supramolecular polymerization (Figure S18b). The absence of excimer emission of **1** and significant fluorescence quenching of **2** due to energy transfer depicts a negligible domain formation of **2** (Figure 4e, S18). Further, the heating curve of the random supramolecular co-polymer showed significantly high stability with a melting temperature (T_m) of 340.2 K, which is 30 K higher than the homo supramolecular polymer of **1** (Figure S19). Finally, the microscopic visualization of these supramolecular polymers showed no distinct red and green emissive fibers and a complete spatial overlap validates the formation of the random supramolecular co-polymers (Figure 4f, S20). We envisage that reactivity ratio (R) ($(R = \Delta G\mathbf{1}\text{-}\mathbf{1}+\Delta G\mathbf{2}\text{-}\mathbf{2})/2\times\Delta G\mathbf{1}\text{-}\mathbf{2}$) of monomers **1** and **2** is 1.02, where disassembled **1** and **2** tend to mix at the level of individual monomers or as small groups of **1** and **2**, leading to an random arrangement of monomers under thermodynamic conditions.[15] This is consistent with the rather similar **1-1** *vs.* **1-2** *vs.* **2-2** monomer-monomer interaction energies obtained from the simulations (Figure 3b) and with the mixing fashion that in such conditions is entropically more favorable (random mixing). This has been further confirmed by means of a coarse-grained molecular dynamics simulation (CG-MD) where 75 + 75 initially disassembled **1** and **2** monomers self-assemble spontaneously during 10 μs of CG-MD in explicit cyclohexane

solvent molecules. During this simulations, **1** and **2** monomers mix in a quite random fashion, where red and green monomers alternate as short segments and/or individual monomers into the generated copolymers as evident from Figure 4g (see also supplementary movies). Notably, the size of the **1** and **2** domains in the mixed stack is related, together with a favored random mixing, in consistent with the fact that **1**-**1** *vs.* **1**-**2** *vs.* **2**-**2** interactions, though very similar, are not perfectly identical. This is also supported by the analysis of the contacts between the centers of the monomer cores (core-core coordination) in the system during the CG-MD simulations (see Figure 4h). In general, a number of contacts equal to 2 identifies a perfect supramolecular polymer, where each monomer has exactly 2 neighbors stably coordinated through their cores. A value of 1 in all curves would mean perfect alternated intermixing of cores. It is interesting to note that in the case where the simulations stat from 75 + 75 initially disassembled monomers, all three red, green and yellow lines tend to equilibrate close to 1, demonstrating the intermixing of small groups (i.e. dimers, trimers, etc.) of red or green is present in the self-assembled structure (in principle, a perfect mixing of alternated **1** and **2** monomers would be compatible with identical red-red, green-green and green-red interaction energies).

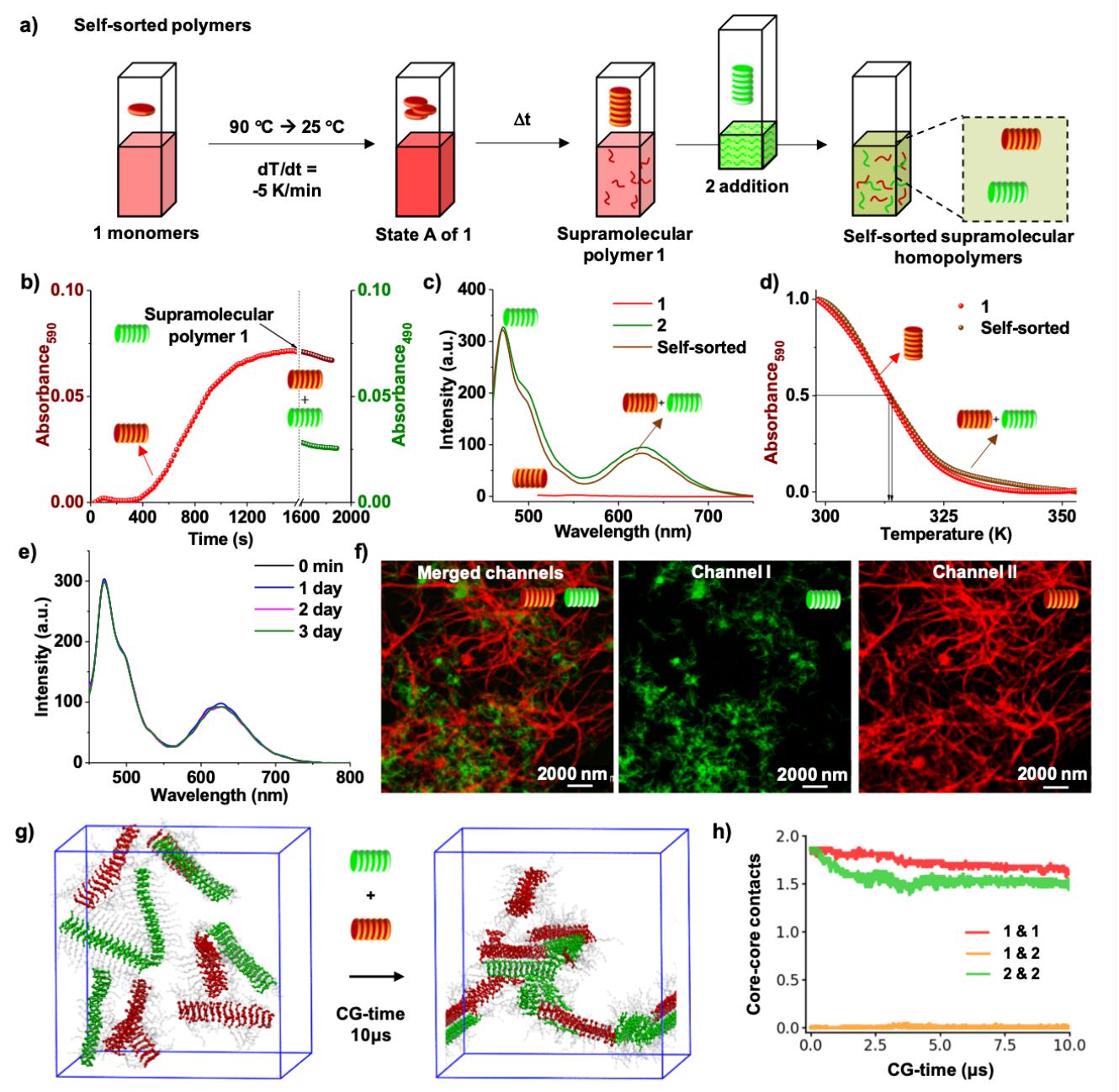

Figure 5. Experimental and computational characterization of narcissistically self-sorted supramolecular homopolymers of **1** and **2**. (a) Schematic representation showing the preparation of the self-sorted homopolymers. (b) Time-dependent absorbance

changes monitored at the aggregate bands of **1** (590 nm) and **2** (490 nm). Addition of supramolecular polymer of **2** to a kinetically grown supramolecular polymer of **1** (after 1600 s), shows insignificant changes in the supramolecular organization of **1** and **2**. (c) Emission spectra of self-sorted and homopolymers of **1** and **2** (λ_{ex} = 442 nm, l = 10 mm), showing negligible energy transfer in the self-sorted state as evident from the lack of quenching of both aggregate and excimer emission of the donor **2** (λ_{ex} = 442 nm, l = 10 mm). (d) The heating curve (monitored with the absorbance at 590 nm) of the solution of self-sorted supramolecular polymers of **1** and **2** showing similar stability of **1** compared to the pure supramolecular polymer of **1** (heating rate = 1 K/min) (e) Time-dependent emission spectra (λ_{ex} = 442 nm, l = 10 mm) of the self-sorted fibers, which does not show any changes with time suggesting the low dynamics of the monomers. (f) Corresponding SIM images showing spatially segregated supramolecular polymers of **1** and **2** confirming the self-sorted arrangement. ([**1**] = [**2**] = 2.5x10^{-5} M, 5 % toluene/MCH, l = 10 mm. (g) Self-assembly of 5 + 5 preformed stacks each containing 15 monomers of **1** and **2** during 10 μs of CG-MD. During the run, the **1** and **2** stacks interact and self-assemble, yet remaining quite stable. (h) Number of contacts between the centers of the red-red (red), green-green (green) and green-red (yellow) monomer cores in the system during the CG-MD – the negligible yellow contacts identify negligible intermixing between the different monomers in the system. (Channel I: λ_{ex} = 488 nm, λ_{coll} = 495–575; Channel II: λ_{ex} = 561 nm, λ_{coll} = 570–650).

mixing would provide a higher *g(c)* peak for the dark-red curve).

These observations show a marked difference from a recent report by Meijer and coworkers, where prevailing homo over heterorecognition leads to the formation of supramolecular block co-polymer under thermodynamic control.[11,15] Altogether our results strongly demonstrate that such different behavior between supramolecular systems based on similar concepts is most likely the consequence of homo *vs.* hetero monomer-monomer interactions in the system. In fact, a perfect segregation in stable blocks starting from disassembled monomers would imply stronger homo vs. hetero monomer-monomer interactions in the system. However, since our current system shows a rather similar hetero vs. homorecognition under thermodynamic conditions, heterogeneous nucleation under kinetic control and at low monomer dynamics (at low temperature) appears to be the only way to obtain supramolecular block co-polymers (vide supra).[20]

Kinetically Stable, Narcissistically Self-Sorted Supramolecular Homopolymers

Supramolecular random co-polymerization under thermodynamic conditions prompted us to investigate the monomer exchange dynamics at room temperature and kinetic stability of the stacks by probing the spectroscopic properties of a mixture of homo-polymers of **1** and **2**. To investigate this, an equimolar mixture of **1** and **2** stacks was synthesized by the post-synthetic mixing of the supramolecular homopolymers of **1** and **2**, made individually by the kinetically controlled nucleation growth (Figure 5a). Independent spectroscopic probing of the **1** and **2** monomers in the homopolymers, did not show any absorbance changes at 590 nm for **1** and 490 nm for **2**, hinting towards the absence of any structural reorganization upon mixing (Figure 5b). Further, the final absorption and CD of this mixture matches well with the summation of the two individual supramolecular polymers (Figure S21), hinting to a self-sorted fibers. In addition, absence of energy transfer depicted by insignificant quenching of donor (**2**) emission in the mixture characterizes that the homopolymers of **1** and **2** are spatially self-sorted (Figure 5c, S22). The heating curves of self-sorted assemblies and individual homostacks match well and show an identical melting temperature (T_m) of 313±1 K reiterating that the supramolecular homopolymers are spatially segregated (Figure 5d, S23). Low exchange dynamics of the monomers at 298 K were further probed via energy transfer for three days, which did not show any change in the emission profile of the donor-acceptor mixture (Figure 5e, S24). These kinetically stable, self-sorted supramolecular homopolymers were microscopically visualized by selective excitation of **1** and **2** (561 nm and 488 nm respectively) using SIM where spatially segregated green and red emissive supramolecular polymers were observed (Figure 5f, S25). This is again consistent with the low monomer exchange dynamics seen for these assemblies from the simulations (Figure 3). This was also further supported by a CG-MD simulation where we inserted 5 + 5 preformed stacks of **1** and **2** monomers, respectively. During the CG-MD run, the stacks were seen to interact in a stable way, but with very limited internal mixing of monomers (Figure 5g, see also supplementary movies). The persistence of the **1** and **2** stacks is also evident in the number of contacts of red and green cores during the CG-MD (close to 2 and minimally changing during the simulation), which means that the fibers are quite ordered and stable and negligible rearrangements in terms of monomer mixing occur in the stacks (Figure 5h).

Supramolecular Block co-polymer under Kinetic Control

Random co-polymerisation of the monomers during the thermodynamic supramolecular co-polymerization (vide supra), suggests that construction of two-component supramolecular block co-polymers requires a kinetically controlled living supramolecular polymerization process. Low monomer exchange dynamics at room temperature, kinetically realizable metastable monomer states, nucleation-growth mechanism of self-assembly and tendency of heterorecognition due to low monomer structural mismatch between **1** and **2**, as evident from the detailed probing of the kinetic and thermodynamic aspects (vide supra) of the monomers, are perfectly suited for the construction of block supramolecular structures via heterogeneous nucleation of the second monomer on the seeds or stacks of the first molecule. Molecule **1** exhibits seeding characteristics as displayed by immediate non-sigmoidal growth of metastable **State A** of **1** upon the addition of pre-grown seeds of **1** during the lag phase (Figure S26).[14] Due to kinetically

controlled nucleation-growth of **1** with a longer lag phase compared to **2**, along with the higher kinetic and thermodynamic stability of **2** (Figure 3), latter was introduced as a seed to the metastable monomers of **1** to trigger the heterogeneous nucleation (Figure S15). A self-assembled segment of monomers **2** (seeds), was synthesized by sonicating a solution of kinetically grown **2** (5×10^{-4} M) for 5 minutes (5 % toluene/MCH) as described in the experimental section. Further metastable state of **1** (**State A**) was synthesized by the fast cooling (5 K/min) of its monomeric solution at 363 K in 5 % toluene/MCH. The addition of seeds of **2** to **State A** of **1** resulted in an instantaneous non-sigmoidal growth depicting heterogeneous nucleation and supramolecular co-polymerization, which is evident from the changes in absorbance monitored selectively at 590 nm corresponding to the aggregate band of **1** (Figure 6b,c). Variation of monomer to seed concentration showed consistent heterogeneous nucleation on the introduction of seed (Figure S27). Increase of monomer concentration with a constant seed concentration showed a linear increase in polymerization rate without any lag phase (Figure 6c, S27a,b). In addition, the variation of seed concentration with constant monomer concentration showed a linear increase in polymerization rate with an increase of seed concentration (Figure S27e,f). These kinetic features refer to the seeded supramolecular polymerization between **1** and **2**.[20] We have ruled out the possibility of secondary nucleation as a side-reaction that competes with seeding to make triblock morphologies by plotting half time of the seeding kinetics against monomer concentration. This was fitted using standard models available to exclude the possibility of any secondary nucleation (Figure S27h).[33] Absorption and CD spectra of the resultant co-assembled solution show that individual aggregation characteristics of both molecules are retained (Figure S27c, d). Further, persistent excimer emission confirms the presence of homopolymeric domains of **2**

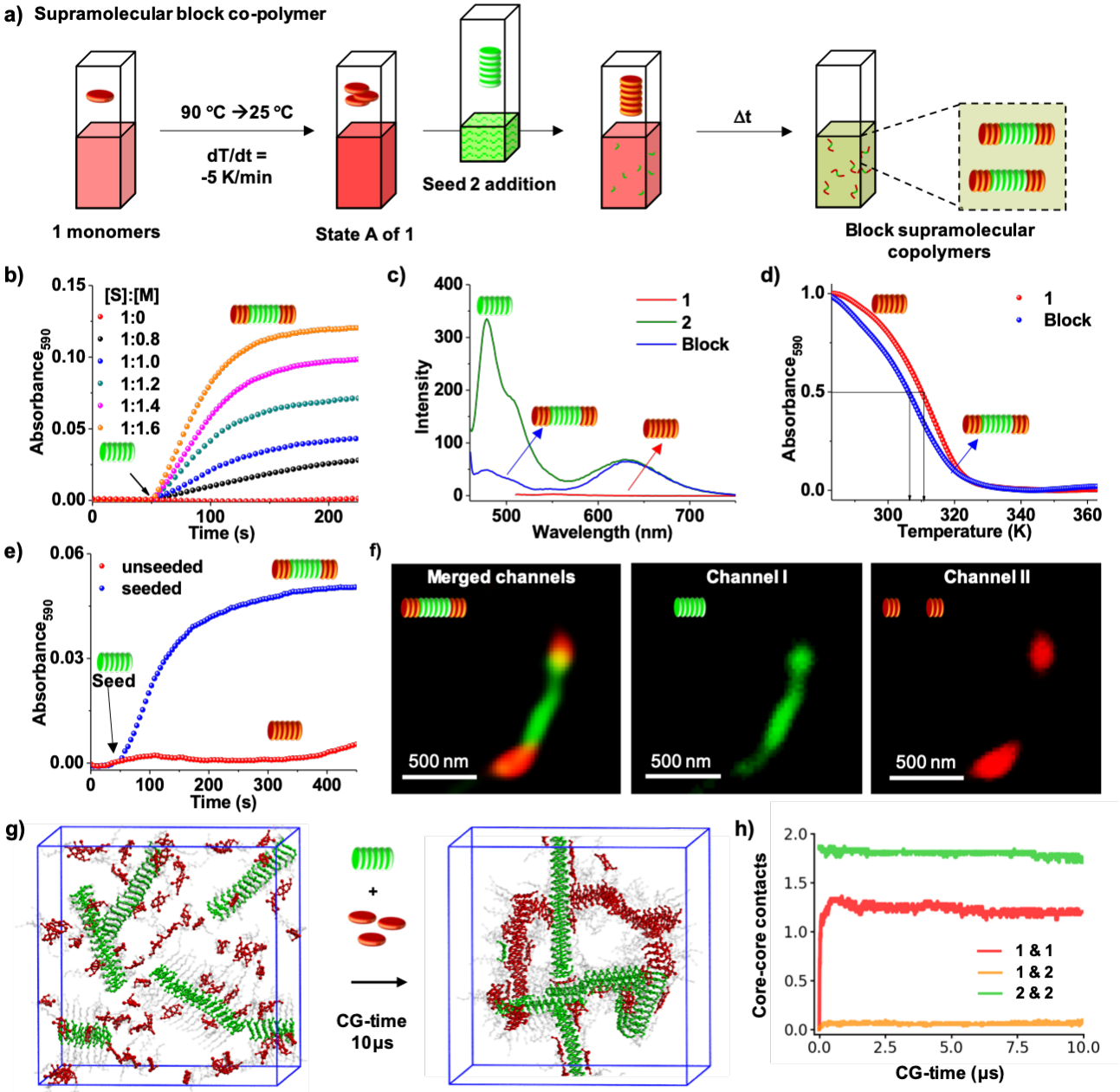

Figure 6. Experimental and computational characterization of heterogeneously seeded supramolecular block co-polymers. (a) Schematic illustration presenting the synthesis of the supramolecular block co-polymers. (b) Time progressive change in absorbance after addition of seeds of **2** (blue curve) at the lag phase of **1** (red curve) monitored at 590 nm (aggregation band of **1**) showing heterogeneous seeding of **1** on **2** supramolecular polymers ([**1**] = [**2**] = 2.5 ×10^{-5} M in the final solution). (c) Time-dependent absorbance changes at 590 nm corresponding to the growth of **1** upon heterogeneous nucleation with constant seed and varying monomer ratio ([**2**] = 2.5 ×10^{-5} M in the final solution). (d) Emission spectra (λ_{ex} = 442 nm) displaying a significant donor emission quenching due to energy transfer from **2** to **1** illustrating an efficient interaction between supramolecular polymers of **1** and **2** and thus suggesting a block formation. (e) Heating curves (1 K/min heating rate) of supramolecular block co-polymer and homopolymer **1** (monitored at aggregate band of **1** at 590 nm), showing a decreased stability of segments of **1** in the co-assembled structure. ([**1**] = [**2**] = 2.5 ×10^{-5} M). (f) SIM images depicting supramolecular block co-polymers ([**1**] = [**2**] = 2.5 ×10^{-5} M, 5 % toluene/MCH). (g) Self-assembly of 75 initially disassembled monomers in the presence of 5 preformed stacks each containing 15 monomers of **2** (seeds) observed during 10 μs of CG-MD. During the run, the **1** monomers self-assemble between them using the **2** stacks as nucleation seeds. (h) (h) Number of contacts between the centers of the red-red (red), green-green (green) and green-red (yellow) monomer cores in the system during the CG-MD – the negligible yellow contacts identify negligible intermixing between the different monomers in the system. (Channel I: λ_{ex} = 488 nm, λ_{coll} = 495–575; Channel II: λ_{ex} = 561 nm, λ_{coll} = 570–650).

in the resultant structure (Figure S28). In addition, the self-assembled emission of **2** at 480 nm is significantly quenched upon co-polymerization, suggesting an efficient energy transfer to **1**, which also hints towards the close proximity of the self-assembled domains of **1** and **2** (Figure 6d, S28). All these observations corroborate to the formation of a supramolecular block co-polymer with an alternating sequence of self-assembled segments of **1** and **2**. The melting curves of the resultant co-assembled stacks showed increased stability of **1** and a negligible difference in the stability of **2** illustrating a block structure (Figure 6e, S29). The supramolecular block co-polymers were visualized by merging green and red emission channels in SIM images showing a spatial correlation of green-emitting fibers terminating with two red-emitting segments (Figure 6f, S30). Due to sonication of supramolecular polymers of **2** to prepare seed, the sizes of final supramolecular block co-polymers are smaller than that of random and self-sorted supramolecular polymers as seen before. Importantly, no significant changes were observed in the spectroscopic features of these block structures, even after 3 days illustrating its low dynamics and high kinetic stability (Figure S31). However, both self-sorted homopolymers and supramolecular block co-polymers, formed under kinetically controlled manner, when heated to 363 K and cooled at 1 K/min, reconfigured to the thermodynamically more stable random supramolecular co-polymers as expected (Figure S32-S33).

These experimental evidences were again supported with molecular simulations. We equilibrated by means of a 10 μs CG-MD simulation a CG system containing 75 initially dispersed monomers of **1** in the presence of 5 preformed stacks of **2** (seeds) similar to a heterogeneous nucleation experiment. In this run, we could observe spontaneous self-assembly of red monomers (**1**) using the green stacks (**2**) as nucleation sites (Figure 6g, see supplementary movies). Thus the simulations show that the self-assembly of **1** is seeded by the assemblies of **2**, in consistent with the experiments. Also, at the same time, this CG-MD shows no appreciable internal rearrangements or dynamic equilibrium of the formed assemblies. While the number of core-core contacts remains nearly constant (close to 2) for the green monomers, the red increases during the CG-MD, but the yellow contacts (indicating intermixing) is close to 0, indicating negligible intermixing of monomers (Figure 6h). This simulation confirms that the **1** monomers indeed self-assemble onto the 2 seeds, but no internal reshuffling of **1** and **2** monomers is evidenced in the generated assemblies in the timescale accessible by these simulations.

Conclusions

In conclusion, through appropriate usage of kinetic and thermodynamic pathway complexity[21] of molecular self-assembly, we have accomplished an unprecedented sequence control in the supramolecular copolymerization of two core-substituted naphthalene diimide π-conjugated monomers to yield self-sorted, random and block supramolecular polymers. Further the characteristic and distinct optical properties of both cNDI monomers which are highly sensitive to the intermolecular interactions along with the induced circular dichroism form the peripheral chiral groups could be explored for the *in situ* spectroscopic probing of the monomer sequence during the kinetically and thermodynamically driven supramolecular co-polymerization process. Further, orthogonal, green and red fluorescence of the monomers **1** and **2** in the supramolecular co-polymers provided a handle to probe the monomer exchange dynamics in the stacks and also helped to uniquely characterize these multi-component structures by visualized under super-resolved structured illumination microscopy. Detailed molecular dynamic simulations provided mechanistic insights into the strength of the inter-monomeric interactions and provided insight into the relative rate of the monomer exchange dynamics in these assemblies, which was crucial for rationalizing the results from heterogenous nucleation experiments. Thermodynamic co-polymerization of monomers **1** and **2** resulted in the random sequence of monomers, due to the comparable **1-1**, **2-2** and **1-2** interaction energies between the monomers. On the other hand, self-sorted homopolymers of **1** and **2** could be realized by exploiting low monomer exchange dynamics or high kinetic stability of these assemblies. Finally, the most challenging block supramolecular co-polymers with domains of **1** and **2** have been synthetized by heterogenous seeded growth.

As mentioned above, the spectroscopic results of the sequence controlled supramolecular co-polymerizations was supported by SIM imaging of the resultant fibers. SIM is ideally suited for the current study as it can visualize the fibers with improved resolution, compared to a standard diffraction-limited microscopy imaging, using the inherent chromophore emission of their monomeric building blocks. While SIM provides an easy to implement a strategy to improve imaging resolution without any perturbation to the monomeric structures, it comes with the caveat of limited improvement in resolution (~120 nm). As a result, a detailed length distribution and yield analysis of the supramolecular block copolymers could not be performed. While other super-resolution imaging strategies can achieve better resolution, they require specialized fluorophores (in case of Stimulated Emission Depletion (STED) or Stochastic Optical Reconstruction Microscopy (STORM)[34,35] or dynamically binding probes (in case of interface point accumulation for imaging in nanoscale topography (PAINT)[36,37] to acquire better-resolved images. The integration of such specialized conditions can lead to significant changes in the mechanism and monomer-exchange dynamics. Hence SIM was the best choice under these circumstances to visualize the resultant fibers and further improvements on the imaging aspects are underway.

Although, sequence-controlled polymers in covalent polymers are defined as sequential positioning of monomers along the polymer backbone[2], here we have utilized the terminology to define the microstructure of a two-component supramolecular co-polymerization.

Synthesis of block-supramolecular structures through kinetically controlled heterogeneous nucleation strategy

presented here is particularly interesting as it is reminiscent of the macro-initiator approach in classical living polymerization by the sequential addition of monomers. This strategy is expected to give pure blocks with a control on the length, compared to the thermodynamically driven cooperative supramolecular co-polymerization based on the reactivity ratio of monomers. We plan to investigate the dispersity and length control of block segments in near future similar to what has been achieved in single component supramolecular polymers.[14,38] Further, supramolecular block co-polymerization of optoelectronically active π-conjugated monomers as described here, would be the way forward to synthesize axial organic heterostructures with a pure donor-acceptor interface to extract interesting functions analogous to well-studied axial inorganic heterostructures. Moving towards higher complexity in terms of multicomponent systems and careful utilization of equilibrium and non-equilibrium states can render much wider regime of structural and functional states of supramolecular polymers.

ASSOCIATED CONTENT

Supporting Information. Extended computational methods and procedures. This material is available free of charge via the Internet at http://pubs.acs.org." For instructions on what should be included in the Supporting Information as well as how to prepare this material for publication, refer to the journal's Instructions for Authors.

AUTHOR INFORMATION

Corresponding Author

*bala@jncasr.ac.in,

*sagasti@jncasr.ac.in,

*giovanni.pavan@polito.it

*george@jncasr.ac.in

Author Contributions

The manuscript was written through contributions of all authors. / All authors have given approval to the final version of the manuscript.

Funding Sources

G. M. P.: Swiss National Science Foundation (SNSF grants IZLIZ_2183336 and 200021_175735) & European Research Council (ERC) under the European Union's Horizon 2020 research and innovation program (grant agreement no. 818776 - DYNAPOL).

ACKNOWLEDGMENT

We would also like to thank JNCASR and the Department of Science and Technology, Government of India, for financial support. In addition, the funding from Sheikh Saqr Laboratory (SSL), JNCASR is also acknowledged. S. J. G. acknowledges the funding received from Nanomission, DST (SR/NM/TP-25/2016), SwarnaJayanti Fellowship Award (DST/SJF/CSA-01/2016-2017) and DBT-JNCASR "Life Science Research, Education and Training at JNCASR" (BT/ INF/22/SP27679/2018). AS and RS thanks CSIR for fellowship. S.S.A. acknowledges SERB Early Career Research Award (Grant ECR/2016/002052) G. M. P. acknowledges the funding received by the Swiss National Science Foundation (SNSF grants IZLIZ2_183336 and 200021_175735) and by the European Research Council (ERC) under the European Union's Horizon 2020 research and innovation program (grant agreement no. 818776 - DYNAPOL).

REFERENCES

1. Berg, J. M.; Tymoczko, J. L.; Stryer, L. *Biochemistry*; 6th edn, W. H. Freeman: New York, 2006.

2. (a) Lutz, J. F.; Ouchi, M.; Liu, D. R.; Sawamoto, M. Sequence-controlled polymers. *Science* **2013**, *341*, 1238149. (b) Lutz, J. F.; Lehn, J-M.; Meijer, E. W.; Matyjaszewski, K. From precision polymers to complex materials and systems. *Nat. Rev. Mater.* **2016**, *1*, 16024-16038.

3. (a) de Greef, T. F. A.; Meijer, E. W. Supramolecular polymers. *Nature* **2008**, *453*, 171-173. (b) Draper, E.R.; Adams, D. J. How should multicomponent supramolecular gels be characterised? *Chem. Soc. Rev.* **2018**, *47*, 3395-3405. (c) Besenius, Pol. Controlling supramolecular polymerization through multicomponent self-assembly. *Polymer Chemistry* **2017**, *55*, 34–78. (d) Vantomme, G.; Meijer, E. W. The construction of supramolecular systems. *Science* **2019**, *363*, 1396-1397.

4. (a) Safont-Sempere, M. M.; Fernández, G.; Würthner, F. self-sorting phenomena in complex supramolecular systems. *Chem. Rev.* **2011**, *111*, 5784-5814. (b) Shigemitsu, H.; Fujisaku, T.; Tanaka, W.; Kubota, R.; Minami, S.; Urayama, K.; Hamachi, I. An adaptive supramolecular hydrogel comprising self-sorting double nanofibre networks. *Nat. Nanotech.* **2018**, *13*, 165–172. (c) Onogi, S.; Shigemitsu, H.; Yoshii, T.; Tanida, T.; Ikeda, M.; Kubota, R.; Hamachi, I. In situ real-time imaging of self-sorted supramolecular nanofibers. *Nat. Chem.* **2016**, *8*, 743 –752.

5. (a) Morris, K. L.; Chen, L.; Raeburn. J.; Sellick, O. R.; Cotanda, P.; Paul, A.; Griffiths, P. C.; King, S.M,; O'Reilly, R. K.; Serpell, L. C.; Adams, D. J. Chemically programmed self-sorting of gelator networks. *Nat. Commun.* **2013**, *4*, 1-6. (b) Draper, E. R.; Eden, E. G. B.; McDonald T. O.; Adams, D. J. Spatially resolved multicomponent gels. *Nat. Chem.* **2015**, *7*, 848–852. (c) Cornwell, D. J.; Daubney, O. J.; Smith, D. K. Photopatterned multidomain gels: multi-component self-assembled hydrogels based on partially self-sorting 1,3:2,4-dibenzylidene-d-sorbitol derivatives. *J. Am. Chem. Soc.* **2015**, *137*, 15486-15492.

6. (a) Prasanthkumar, S.; Ghosh, S.; Nair, V. C.; Saeki, A.; Seki, S.; Ajayaghosh, A. Organic donor-acceptor assemblies form coaxial p-n heterojunctions with high photoconductivity. *Angew. Chem., Int. Ed.* **2015**, *54*, 946–950. (b) Sandeep, A.; Praveen, V. K.; Kartha, K. K.; Karunakaranab, V.; Ajayaghosh, A. Supercoiled fibres of self-sorted donor–acceptor stacks: a turn-off/turn-on platform for sensing volatile aromatic compounds. *Chem. Sci.* **2016**, *7*, 4460. (c) Herrikhuyzen, J. v.; Syamakumari, A.; Schenning, A. P. H. J.; Meijer, E. W. Synthesis of n-Type perylene bisimide derivatives and their orthogonal self-assembly with p-Type oligo(p-phenylene vinylene)s. *J. Am. Chem. Soc.* **2004**, *126*, 10021–10027.

7. (a) Narayan, B.; Bejagam, K. K.; Balasubramanian, S.; George, S. J. Autoresolution of segregated and mixed p-n stacks by stereoselective supramolecular polymerization in solution. *Angew. Chem., Int. Ed.* **2015**, *54*, 13245–13249. (b) Sarkar, A.; Dhiman, S.; Chalishazar, A.; George, S. J. Visualization of stereoselective supramolecular polymers by chirality-controlled energy transfer. *Angew. Chem., Int. Ed.* **2017**, *56*, 13767 –13771.

8. (a) Zhang, X.; Wang, C. Supramolecular amphiphiles. *Chem. Soc. Rev.* **2011**, *40*, 94-101. (b) Wang, C.; Guo, Y.; Wang, Y.; Xu, H.; Wang, R.; Zhang, X. Supramolecular amphiphiles based on a water-soluble charge-transfer complex: fabrication of ultralong nanofibers with tunable straightness. *Angew. Chem., Int. Ed.* **2009**, *48*, 8962–896. (c) Kumar, M.; Rao, K. V.; George, S. J. Supramolecular

charge transfer nanostructures. *Phys. Chem. Chem. Phys.* **2014**, *16*, 1300-1313. (d) Rao, K. V.; Jayaramulu, K.; Maji, T. K.; George, S. J. Supramolecular hydrogels and high-aspect-ratio nanofibers through charge-transfer-induced alternate coassembly. *Angew. Chem., Int. Ed.* **2010**, *49*, 4218-4222.

9. (a) Frisch, H.; Unsleber, J. P.; Lgdeker, D.; Peterlechner, M.; Brunklaus, G.; Waller, M.; Besenius, P. pH-Switchable ampholytic supramolecular copolymers. *Angew. Chem., Int. Ed.* **2013**, *52*, 10097–10101. (b) Frisch, H.; Fritz, E.; Stricker, F.; Schmüser, L.; Spitzer, D.; Weidner, T.; Ravoo, B. J.; Besenius, P. Kinetically controlled sequential growth of surface-grafted chiral supramolecular copolymers. *Angew. Chem., Int. Ed.* **2016**, *55*, 7242 – 7246.

10. Appel, E. A.; Biedermann, F.; Rauwald, U.; Jones, S. T.; Zayed, J. M.; Scherman, O. A. Supramolecular cross-linked networks via host-guest complexation with cucurbit[8]uril. *J. Am. Chem. Soc.* **2010**, *132*, 14251.

11. (a) Adelizzi, B.; Van Zee, N. J.; De Windt, L. N.; Palmans, A. R.; Meijer, E. W. Future of supramolecular copolymers unveiled by reflecting on covalent copolymerization. *J. Am. Chem. Soc.* **2019**, *141*, 6110-6121. (b) Wehner, M.; Würthner, F. Supramolecular polymerization through kinetic pathway control and living chain growth. *Nat. Rev. Chem.* **2019**, *4*, 38-53. (c) Jain, A.; George, S. J. New directions in supramolecular electronics. *Mater. Today*, **2015**, *18*, 206-214.

12. (a) Jonkheijm, P.; van der Schoot, P.; Schenning, A. P. H. J.; Meijer, E. W. Probing the solvent-assisted nucleation pathway in chemical self-assembly. *Science* **2006**, *313*, 80-83**.** (b) De Greef, T. F. A.; Smulders, M. M. J.; Wolffs, M.; Schenning, A. P. H. J.; Sijbesma, R. P.; Meijer, E. W. Supramolecular polymerization. *Chem. Rev.* **2009**, *109*, 5687–5754. (c) Kulkarni, C.; Balasubramanian, S.; George, S. J. What molecular features govern the mechanism of supramolecular polymerization? *ChemPhysChem* **2013**, *14*, 661 – 673.

13. (a) Dhiman, S.; George, S. J. Temporally controlled supramolecular polymerization. *Bull. Chem. Soc. Jpn.* **2018**, *91*, 687-699. (b) van der Zwaag, D.; De Greef, T. F. A.; Meijer, E. W. Programmable supramolecular polymerizations. *Angew. Chem., Int. Ed.* **2015**, *54*, 8334–8336. (c) Mukhopadhyay, R. D.; Ajayaghosh, A. Living supramolecular polymerization, *Science* **2015**, *349*, 241. (d) Matern, J.; Dorca, Y.; Sánchez, L.; Fernández, G. Revising complex supramolecular polymerization under kinetic and thermodynamic control. *Angew. Chem., Int. Ed.* **2019**, *58*, 16730-16740.

14. (a) Fukui, T.; Kawai, S.; Fujinuma, S.; Matsushita, Y.; Yasuda, T.; Sakurai, T.; Seki, S.; Takeuchi, M.; Sugiyasu, K. Control over differentiation of a metastable supramolecular assembly in one and two dimensions. *Nat. Chem.* **2017**, *9*, 493-499. (b) Ogi, S.; Sugiyasu, K.; Manna, S.; Samitsu, S.; Takeuchi, M. Living supramolecular polymerization realized through a biomimetic approach. *Nat. Chem.* **2014**, *6*, 188-195. (c) Ogi, S.; Stepanenko, V.; Sugiyasu, K.; Takeuchi, M.; Würthner, F. Mechanism of self-assembly process and seeded supramolecular polymerization of perylene bisimide organogelator. *J. Am. Chem. Soc.* **2015**, *137*, 3300-3307. (d) Ogi, S.; Stepanenko, V.; Thein, J.; Würthner, F. Impact of alkyl spacer length on aggregation pathways in kinetically controlled supramolecular polymerization. *J. Am. Chem. Soc.* **2016**, *138*, 670-678. (e) Endo, M.; Fukui, T.; Jung, S. H.; Yagai, S.; Takeuchi, M.; Sugiyasu, K. Photoregulated living supramolecular polymerization established by combining energy landscapes of photoisomerization and nucleation–elongation processes. *J. Am. Chem. Soc.* **2016**, *138*, 14347–14353. (f) Kemper, B.; Zengerling, L.; Spitzer, D.; Otter, R.; Bauer, T.; Besenius, P. Kinetically controlled stepwise self-assembly of AuI-metallopeptides in water. *J. Am. Chem. Soc.* **2018**, *140*, 2, 534-537. (g) Ogi, S.; Matsumoto, K.; Yamaguchi, S. Seeded polymerization through the interplay of folding and aggregation of an amino-acid-based diamide. *Angew. Chem., Int. Ed.* **2018**, *57*, 2339–2343. (h) Greciano, E. E.; Matarranz, B.; Sánchez, L. Pathway complexity versus hierarchical self-assembly in N-annulated perylenes: Structural effects in seeded supramolecular polymerization. *Angew. Chem., Int. Ed.* **2018**, *57*, 4697–4701. (i) Robinson, M. E.; Lunn, D. J.; Nazemi, A.; Whittell, G. R.; De Cola, L.; Manners, I. *Chem. Commun.*, **2015**, *51*, 15921-15924.

15. Adelizzi, B.; Aloi, A.; Markvoort, A. J.; Ten Eikelder, H. M.; Voets, I. K.; Palmans, A. R.; Meijer, E. W. Supramolecular block copolymers under thermodynamic control. *J. Am. Chem. Soc.* **2018**, *140*, 7168-7175.

16. Kitamoto, Y.; Pan, Z.; Prabhu, D. D.; Isobe, A.; Ohba, T.; Shimizu, N.; Takagi, H.; Haruki, R.; Adachi, S. I.; Yagai, S. One-shot preparation of topologically chimeric nanofibers via a gradient supramolecular copolymerization. *Nat. Commun.* **2019**, *10*, 4578.

17. (a) Jung, S. H.; Bochicchio, D.; Pavan, G. M.; Takeuchi, M.; Sugiyasu, K. A block supramolecular polymer and its kinetically enhanced stability. *J. Am. Chem. Soc.* **2018**, *140*, 10570-10577.

18. (a) Wang, X.; Guerin, G.; Wang, H.; Wang, Y.; Manners, I.; Winnik, M. Cylindrical block copolymer micelles and co-micelles of controlled length and architecture. *Science* **2007**, *317*, 644–648. (b) Gilroy, J. B.; Gädt, T.; Whittell, G. R.; Chabanne, L.; Mitchels, J. M.; Richardson, R. M.; Winnik, M. A.; Manners, I. Monodisperse cylindrical micelles by crystallization-driven living self-assembly. *Nat. Chem.* **2010**, *2*, 566–570. (c) Finnegan, J. R.; Lunn, D. J.; Gould, Z. M. Hudson, O. E. C.; Whittell, G. R.; Winnik, M. A.; Manners, I. Gradient crystallization-driven self-assembly: cylindrical micelles with "patchy" segmented coronas via the coassembly of linear and brush block copolymers. *J. Am. Chem. Soc.* **2014,** *136, 13835-13844*. (d) Schacher, F. H.; Rupar, P. A.; Manners. I. Functional block copolymers: nanostructured materials with emerging applications. *Angew. Chem., Int. Ed.* **2012**, *51*, 7898-7921. (e) Qiu, H.; Gao, Y.; An Du, V.; Harniman, R.; Winnik, M. A.; Manners, I. Branched micelles by living crystallization-driven block copolymer self-assembly under kinetic control. *J. Am. Chem. Soc.* **2015**, *137*, 2375–2385.

19. Zhang, W.; Jin, W.; Fukushima, T; Saeki, A.; Seki, S.; Aida, T. Supramolecular linear heterojunction composed of graphite-like semiconducting nanotubular segments. *Science* **2011**, *334,* 340-343.

20. (a) Görl, D.; Zhang, X.; Stepanenko, V.; Würthner, F. Supramolecular block copolymers by kinetically controlled co-self-assembly of planar and core-twisted perylene bisimides. *Nat. Commun.* **2015**, *6*, 7009. (b) Wagner, W.; Wehner, M.; Stepanenko, V.; Würthner, F. Supramolecular block copolymers by seeded living polymerization of perylene bisimides. *J. Am. Chem. Soc.* **2019**, *141*, 12044-12054.

21. (a) Korevaar, P. A.; de Greef, T. F. A.; Meijer, E. W. Pathway complexity in π-conjugated materials. *Chem. Mater.* **2014**, *26*, 576–586. (b) Korevaar, P. A.; George, S. J.; Markvoort, A. J.; Smulders, M. M.; Hilbers, P. A.; Schenning, A. P.; de Greef, T. F. A.; Meijer, E. W. Pathway complexity in supramolecular polymerization. *Nature* **2012**, *481*, 492–496. (c) Langenstroer, A.; Kartha, K. K.; Dorca, Y.; Droste, J.; Stepanenko, V.; Albuquerque, R. Q.; Hansen, M. R.; Sánchez, L.; Fernández G. Unraveling concomitant packing polymorphism in metallosupramolecular polymers. *J. Am. Chem. Soc.* **2019**, *141*, 5192–5200.

22. (a) Kulkarni, C.; Bejagam, K. K.; Senanayak, P. S.; Narayan, K. S.; Balasubramanian, S.; George, S. J. Dipole-moment-driven cooperative supramolecular polymerization. *J. Am. Chem. Soc.* **2015**, *137*, 3924-3932. (b) Kulkarni, C.; George, S. J. Carbonate Linkage Bearing Naphthalenediimides: Self-assembly and photophysical properties. *Chem. Eur. J.* **2014**, *16*, 4537-4541.

23. (c) George, S. J.; Tomović, Ž.; Schenning, A. P. H. J.; Meijer, E. W. Insight into the chiral induction in supramolecular stacks through preferential chiral solvation. *Chem. Commun.* **2011**, *47*, 3451-3453. (d) Cat, I. D.; Guo, Z.; George, S. J.; Meijer, E. W.; Schenning, A. P. H. J.; Feyter, S. D. Induction of chirality in an achiral

monolayer at the liquid/solid interface by a supramolecular chiral auxiliary. *J. Am. Chem. Soc.* **2012**, *134*, 3171-3177.
24. Kubota, R.; Nakamura, K.; Torigoe, S.; Hamachi, I. The Power of Confocal Laser Scanning Microscopy in Supramolecular Chemistry: In situ real-time imaging of stimuli-responsive multicomponent supramolecular hydrogels. *ChemistryOpen* **2020**, *9*, 67–79.
25. Bochicchio, D.; Pavan. G. M. Molecular modelling of supramolecular polymers. *Adv. Phys. X* **2018**, *3*, 1436408.
26. Bochicchio, D.; Pavan. G. M. From cooperative self-assembly to water-Soluble supramolecular polymers using coarse-grained simulations. *ACS Nano* **2017**, *11*, 1000-1011.
27. Gasparotto, P.; Bochicchio, D.; Ceriotti, M.; Pavan, G. M. Identifying and tracking defects in dynamic supramolecular polymers. *J. Phys. Chem. B* **2020**, *124*, 589-599.
28. Bochicchio, D.; Salvalaglio, M.; Pavan, G. M. Into the dynamics of a supramolecular polymer at submolecular resolution. *Nat. Commun.* **2017**, *8*, 147
29. Marrink, S. J.; Risselada, H. J.; Yefimov, S.; Tieleman, D. P.; de Vries, A. H. The MARTINI force field: coarse grained model for biomolecular simulations *J. Phys. Chem. B.* **2007**, *111*, 7812–7824.
30. Barducci, A., Bussi, G.; Parrinello, M. Well-tempered metadynamics: a smoothly converging and tunable free-energy method. *Phys. Rev. Lett.* **2008**, *100*, 020603.
31. Tiwary, P.; Parrinello, M. From metadynamics to dynamics. *Phys. Rev. Lett.* **2013**, *111*, 230602.
32. Salvalaglio, M.; Tiwary, P.; Parrinello, M. Assessing the reliability of the dynamics reconstructed from metadynamics. *J. Chem. Theory Comput.* **2014**, *10*, 1420–1425.
33. (a) Meisl, G.; Kirkegaard, J. B.; Arosio, P.; Michaels, T. C. T.; Vendruscolo, M.; Dobson, C. M.; Linse, S.; Knowles, T. P. J. Molecular mechanisms of protein aggregation from global fitting of kinetic models. *Nat. Protoc.* **2016**, *11*, 252-272. (b) Iglesias, J. L.; Tassoni, A.; Adachi, T.; Stich, M.; Hermans, T. M. Oscillations, travelling fronts and patterns in a supramolecular system. *Nat. Nanotech.* **2018**, *13*, 1021–1027.
34. Vicidomini, G.; Bianchini, P.; Diaspro, A. STED super-resolved microscopy.Nat. Methods **2018**, *15*, 173-182.
35. Albertazzi, L.; van der Zwaag, D.; Leenders, C. M. A.; Fitzner, R.; van der Hofstad, R. W.; Meijer, E. W. Probing Exchange Pathways in One-Dimensional Aggregates with Super-Resolution Microscopy. *Science* **2014**, *344*, 491–495.
36. Adelizzi, B.; Aloi, A.; Van Zee, N. J.; Palmans, A. R. A.; Meijer, E. W.; Voets, I. K. Painting Supramolecular Polymers in Organic Solvents by Super-resolution Microscopy. *ACS Nano* **2018**, *12*, 4431–4439.
37. Sasmal, R.; Saha, N. D.; Schueder, F.; Joshie, D.; Sheeba, V.; Jungmann, R.; Agasti. S. S. 4. Dynamic host–guest interaction enables autonomous single molecule blinking and super-resolution imaging. *Chem. Commun.*, **2019**, *55*, 14430-14433.
38. (a) Vázquez-González, V.; Mayoral, M. J.; Chamorro, R.; Hendrix, M. M.R.M.; Voets, I. K.; Gonzalez-Rodriguez, D. Noncovalent synthesis of self-assembled nanotubes through decoupled hierarchical cooperative processes. *J. Am. Chem. Soc.* **2019**, *141*, 16432-16438. (b) Bousmail, D.; Chidchob, P.; Sleiman, H. F. Cyanine-mediated DNA nanofiber growth with controlled dimensionality. *J. Am. Chem. Soc.* **2018**, *140*, 9518-9530.

Insert Table of Contents artwork here

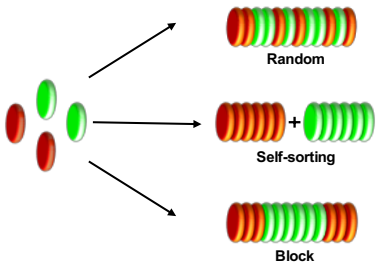

Sequence Controlled Supramolecular Polymerization